Solar Energy Materials & Solar Cells 120 (2014) 642–646

Contents lists available at ScienceDirect

Solar Energy Materials & Solar Cells

journal homepage: www.elsevier.com/locate/solmat

Current–voltage characteristics of fully solution processed high performance $CuIn(S,Se)_2$ solar cells: Crossover and red kink

Choong-Heui Chung [a,b], Brion Bob [a], Tze-Bin Song [a], Yang Yang [a,*]

[a] Department of Materials Science and Engineering and California NanoSystems Institute, University of California Los Angeles, Los Angeles, CA 90095, USA
[b] Department of Materials Science and Engineering, Hanbat National University, Daejeon 305-719, Korea

ARTICLE INFO

Article history:
Received 7 June 2013
Accepted 16 October 2013
Available online 9 November 2013

Keywords:
Thin film solar cells
Crossover
Red kink
Nanowire

ABSTRACT

We recently reported the successful replacement of both sputtered intrinsic zinc oxide (i-ZnO) and sputtered indium tin oxide (ITO) window layers by a solution processed silver nanowire composite window (SNCW) layer for fully solution processed high performance $CuIn(S,Se)_2$ (CISS) thin film solar cells without any sacrifices in photovoltaic device performance. Here, we report the current density–voltage (*J–V*) characteristics of the fully solution processed CISS thin film solar cells with the SNCW layer under dark conditions, and under white and filtered red-light illumination. While control devices with sputtered conductive metal oxide window layers do not show *J–V* distortion, devices with the SNCW exhibit both crossover and red kink behaviors, which disappear during white-light illumination but gradually re-appear after turning off light. We propose the following model to explain the above observations. Acceptor-like defects at the CdS/SNCW interface become negatively charged by capturing electrons under dark conditions, but are neutralized by capturing photo-generated holes from the CdS valence band under white-light illumination. The illumination dependent state of the acceptor-like defects leads to the appearance and disappearance of the crossover and red kink from the *J–V* curves.

1. Introduction

The use of vacuum deposition methods in the preparation of chalcogenide absorber layer and intrinsic and n-type metal oxide window layers has produced highly efficient $Cu(In,Ga)Se_2$ (CIGS) photovoltaic devices [1,2]. However, non-vacuum methods have been continuously researched for the purpose of cost reduction as well as the large scale production of solar modules that are able to compete with conventional electric power generation [3–7]. We recently reported fully solution processed high performance $CuIn(S,Se)_2$ (CISS) thin films solar cells that employ hydrazine solution-processed absorber layers and silver nanowire composite window (SNCW) layers [8]. The SNCW layer consists of a discrete silver nanowire network encased within a moderately conductive metal oxide nanoparticle matrix. The silver nanowire mesh provides low sheet resistance, and the conductive metal oxide nanoparticles fill the voids present between silver nanowires to offer a path for carrier transport between individual wires, effectively replacing both the conventional intrinsic zinc oxide (i-ZnO) and indium tin oxide (ITO) layers. The photovoltaic performances of CISS solar cells employing the SNCW layer were comparable to or even better than those of control devices using conventional sputtered i-ZnO/ITO. In order to further improve this window layer for a wider range of photovoltaic device applications, a deeper understanding of carrier transport behaviors in the device structures utilizing the SNCW will be necessary.

In standard CI(G)S devices with conventional sputtered metal oxide window layers, distortion in the current density–voltage (*J–V*) curve can be caused by non-Ohmic back-contact [9], and deep level defects in the CIGS absorber [10,11], in the CdS buffer layer [12–15], and at the absorber/buffer interface [11–15]. In this work, we observed that while our control CISS devices with a conventional sputtered i-ZnO/ITO window layer did not show any *J–V* distortion, our CISS devices utilizing the SNCW layers showed both crossover and red kink in *J–V* characteristics. The existence of acceptor-like deep level defects at the CdS/SNCW interface in the Mo/CISS/CdS/SNCW photovoltaic devices may lead to both crossover and red kink behavior, which are removed when illuminating with white-light, but gradually re-appear after the illumination is turned off.

2. Background

2.1. Band alignment and barrier for diode current and photo-current

Carrier transport behavior is strongly affected by band alignment in semiconductor device structures. Fig. 1 shows a schematic of the

* Correspondence to: Dept of Materials Science and Engineering, University of California Los Angeles, Engineering V Building, 420 Westwood Plaza, Los Angeles, CA 90095 (USA). Tel.: +1 310 825 4052; fax: +1 310 825 3665.
E-mail address: yangy@ucla.edu (Y. Yang).

0927-0248/$ - see front matter © 2013 Elsevier B.V. All rights reserved.
http://dx.doi.org/10.1016/j.solmat.2013.10.013

conduction-band minimum E_C of the CISS/CdS/SNCW structure at zero bias with a spike type CISS/CdS junction. In Fig. 1, V_{CISS}, V_{CdS} and V_W are the band bending potentials in the CISS, CdS, and window layer, respectively. ΔE_C^{ab} and ΔE_C^{bw} are the conduction band discontinuities between the CISS and CdS, and between the CdS and window layer, respectively. ΔE_{Fn} is the difference between the conduction band edge of the CISS and the electron quasi-Fermi level at the CdS/CISS interface.

Injected electrons from the top electrode have to surmount the energy barrier $\varnothing_b^n$ to be collected as diode current which exponentially decreases with increasing $\varnothing_b^n$ values [16,17]. Decreased band bending in the window layer and/or CdS under white-light illumination can lead to crossover of the dark J–V and white-light J–V curves because the electron barrier $\varnothing_b^n$ is the sum of ΔE_C^{bw}, V_{CdS} and V_W (Fig. 1). A kink in the J–V curve results from a limited thermionic emission current over the energy barrier ΔE_C^{ab}. Once photo-generated electrons in the CISS reach the CISS/CdS interface, they must surmount the energy barrier ΔE_C^{ab} by thermionic emission in order to be collected as photocurrent (Fig. 1). Thus, as long as the thermionic emission current over the barrier is much larger than the number of photo-generated electrons approaching the junction, the conduction band barrier will have a negligible influence on the total photocurrent collected from the device. Current passing through the barrier by thermionic emission is linearly dependent on the electron concentration at the CISS/CdS interface [17,18]. This electron concentration exponentially increases with V_{CISS} which is reduced by applying a forward bias. Thus, the smaller values of V_{CISS} at zero bias can lead to a kink in J–V.

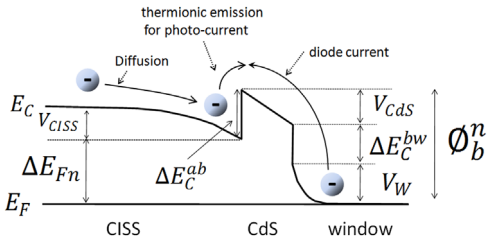

Fig. 1. Conduction band minimum E_C alignment in the structure of CISS/CdS/window, and electron flows along energy band and their energy barrier for photo-current and diode current.

3. Experiment

3.1. Device fabrication

We deposited the SNCW layer onto the structure CdS (30 nm)/CISS (1500 nm)/Mo (350 nm)/glass to complete the devices (Fig. 2(a)). The SNCW was prepared by the sequential spin-coating of silver nanowires and indium tin oxide nanoparticles. A control device with a conventional sputtered i-ZnO(30 nm)/ITO(150 nm) electrode

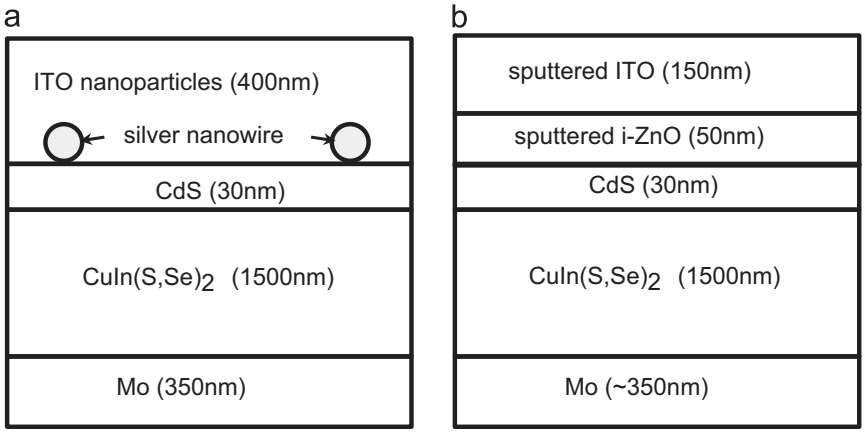

Fig. 2. Structure of a CISS device with SNCW layer composed of silver nanowires embedded in indium tin oxide nanoparticles. (b) Control device with a sputtered i-ZnO/ITO window layer.

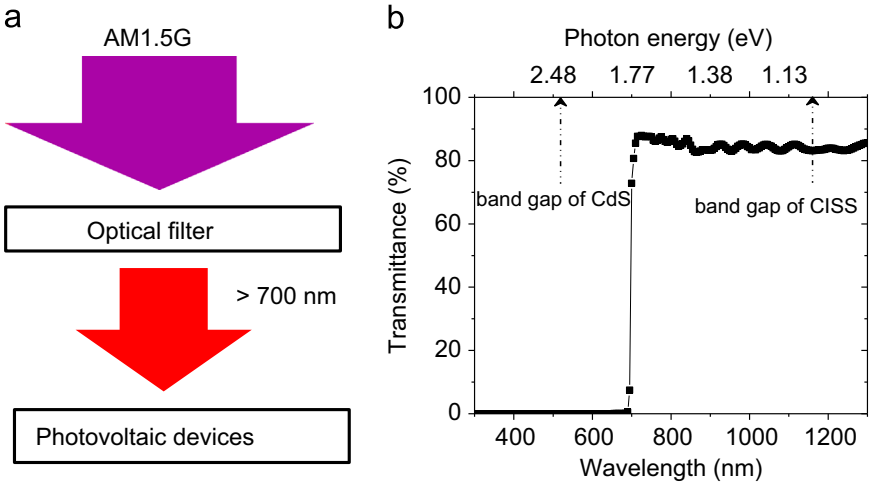

Fig. 3. (a) Set-up for red J–V measurement. Optical filter is placed just above samples cut off light with wavelength less than 700 nm. (b) Optical transmittance of the filter used for red J–V measurement. (For interpretation of the references to color in this figure legend, the reader is referred to the web version of this article.)

was also fabricated for comparison (Fig. 2(b)). Mo thin films were deposited on soda–lime glass using direct current magnetron sputtering. CISS and CdS layers were then sequentially prepared by hydrazine solution processing and chemical bath deposition, respectively. Fabrication details can be found elsewhere in our previous works [8,19–22].

3.2. *J–V* measurements

The *J–V* characteristics of the fabricated devices were measured using a Keithley 2400 power supply under dark, red-light illumination and white-light illumination. Dark *J–V* and red *J–V* curves were measured before and after white-light illumination to investigate the *J–V* dependence on white light. White-light illumination was obtained by a simulated AM1.5G spectrum with a power density of 100 mW/cm^2 provided by an Oriel 91191 solar simulator. For red *J–V* measurements, a 700 nm (1.77 eV) long pass optical filter was placed just above the photovoltaic devices to remove photons with higher energy than the energy band gap of the CdS layer (2.4 eV) from the AM1.5G spectrum (Fig. 3(a)). The transmittance of the optical filter is approximately 85% above the 700 nm region and ~0% at wavelengths below the 700 nm region (Fig. 3(b)). Thus, measurement conditions for the red *J–V* forbid the photo-generation of electron–hole pairs in the CdS layer.

4. Results and discussion

4.1. Crossover and red kink

Fig. 4 shows dark *J–V* and red *J–V* curves before and after white-light illumination and the white-light *J–V* curves of devices with SNCW layers and sputtered i-ZnO/ITO control devices. The device with the SNCW clearly shows a crossover of the dark *J–V* and the white-light *J–V* at voltages slightly above open circuit voltage (Fig. 4(a) and (b)) while the control device with a sputtered i-ZnO/ITO showed no such distortion both before and after white-light illumination (Fig. 4(c) and (d)). Under red-light illumination in the device with the SNCW, we observed a good collection of photo-current only below 0.1 V, reduced photo-current collection in the range from 0.2 V to 0.4 V, and almost no collection of photo-current collection in the range above 0.4 V. Impeded photo-current collection below the open circuit voltage significantly decreases the fill factor (FF) of photovoltaic device. This observation is typically referred to as the red kink. Both *J–V* distortions disappeared after shining white-light on the device, but gradually re-appeared after the illumination was turned off.

4.2. Proposed transport and collection model

Based on above experimental observations and the expected band alignments that may lead to crossover and red kink, we propose the existence of acceptor-like deep level defects at the CdS/SNCW interface. Under dark conditions, these deep level interfacial defects are mostly occupied by electrons supplied by the n-type adjacent layers (Fig. 5(a)) resulting in negative area charge at the CdS/SNCW interface and a positive space charge region in the SNCW. This charge distribution allocates less space charge inside the CISS layer [17]. As a result, the magnitude of the V_{CISS} value is reduced while V_W increases (Fig. 5(b)), which in turn can lead to crossover and red kink through the mechanisms explained earlier during the band alignment discussion. Once white-light illuminates devices with an SNCW, high energy blue photons generate electron–hole pairs in the CdS layer. Photo-generated holes then attempt to occupy the negatively charged interface defects by competing against electrons present near the interface, which includes photo-generated electrons within the CdS layer and electrons in the adjacent SNCW. In general, acceptor-like defects have larger capture cross-section for holes when they are negatively charged than for electrons when they are neutralized [12]. Therefore, the negatively charged acceptor-like

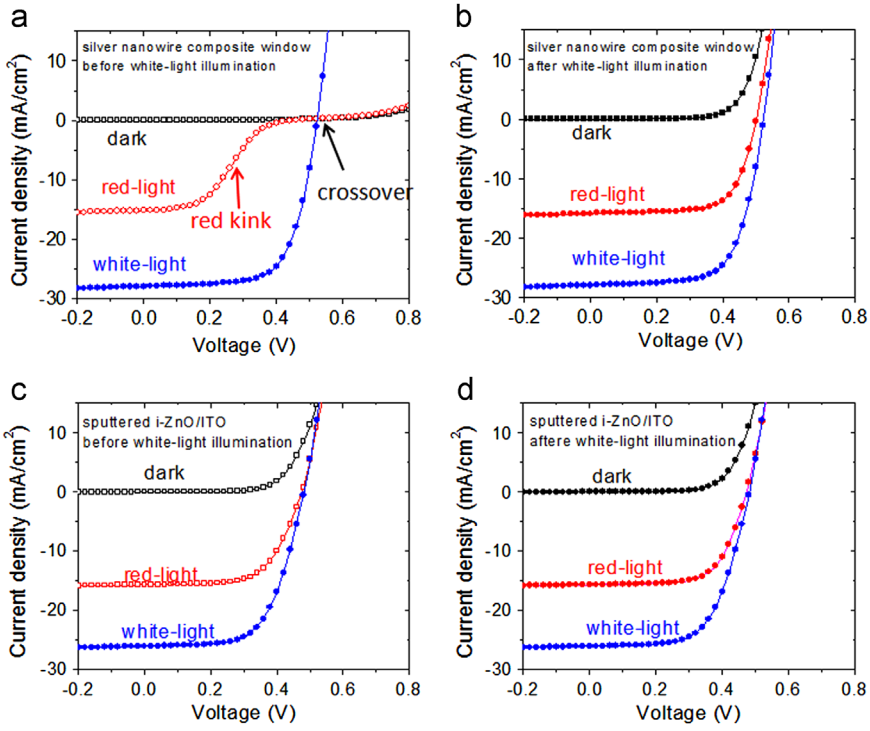

Fig. 4. Dark *J–V* and red *J–V* (a) before and (b) after white-light illumination, and white-light *J–V* of CISS device with SNCW. Dark *J–V* and red *J–V* (c) before and (d) after white-light illumination. Crossover and red kink are observed only in CISS devices with SNCW before white-light illumination. (For interpretation of the references to color in this figure legend, the reader is referred to the web version of this article.)

defects are largely neutralized under white-light illumination by capturing holes present in the CdS layer. As a result, the V_{CISS} value is increased and the V_W value is decreased (Fig. 5(b)) which in turn lead to the disappearance of both crossover and red kink.

After turning-off white-light, the CdS layer can no longer sustain an appropriate concentration of photo-generated holes. Most interfacial defects are then re-occupied by electrons, which leads to the re-appearance of *J–V* distortions. In other words, the charge state of the acceptor-like defects at the CdS/SNCW interface is dependent on the concentration of electrons and holes in each of the adjacent layers, and the capture cross-section for holes and electrons. Under dark conditions, the electron concentration is much larger than that of holes in the n-type buffer and window layers, and therefore electrons occupy most of the defects. Under illumination, the concentration of hole becomes more comparable to that of electrons and the capture cross-section for hole remains much larger than that of electron. Thus, most electrons located at defects recombine with holes resulting in neutralization of the defects.

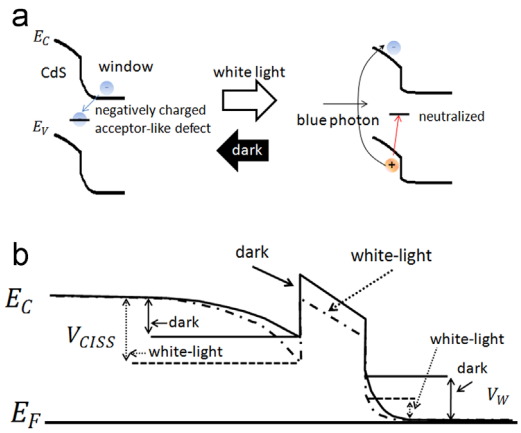

Fig. 5. (a) Acceptor-like deep level defects at the CdS/SNCW interface become negatively charged by capturing electrons from n-type window layer under dark, and are neutralized by capturing photo-generated holes in the CdS under white-light illumination. (b) Resulting E_C alignment under dark and after white-light illumination. Band-bending in the CISS and window layers is increased and decreased upon white-light illumination, respectively. (For interpretation of the references to color in this figure legend, the reader is referred to the web version of this article.)

4.3. Response time

To investigate the response speed of the acceptor-like defects located at the CdS/SNCW interface, we measured red *J–V* curves as a function of white-light illumination time and as a function of time after turning off white-light. The measurement of red *J–V* distortion ΔV was defined by the voltage difference between distorted red *J–V*s and a fully recovered red *J–V* at half of the short circuit current density (J_{SC}). Red kinks were fully removed from the *J–V* curve after only 10 s of white-light illumination (Fig. 6 (a) and (b)), while it took approximately 1000 s to completely relax back to the maximum red *J–V* distortion (Fig. 6(c) and (d)). This is a reasonable result, as we can expect the time constant for creating the red kink to be inversely related to the capture cross-section for electron by neutralized acceptor-like defects and the time constant for removing it to be inversely related to the capture cross-section for holes by negatively charged acceptor-like defects. The general nature of acceptor-like defects, which is to exhibit a significantly larger capture cross-section for holes when they are negatively charged than for electrons when they are neutral, results in a factor of 100 difference in time constant between formation and removal

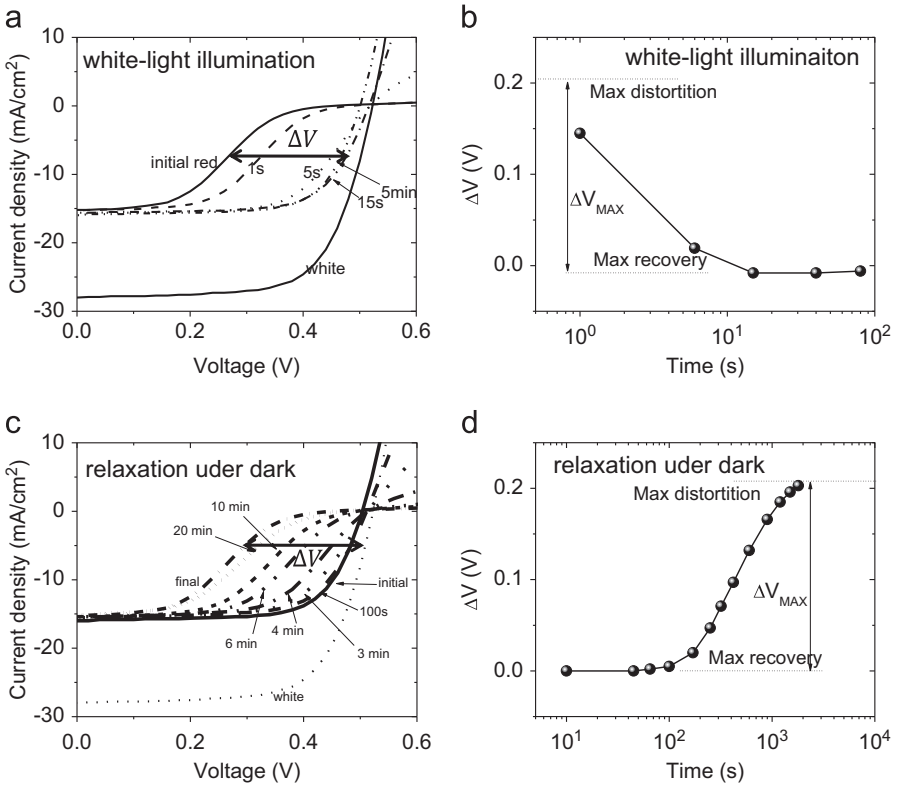

Fig. 6. (a) Red *J–V* and (b) degree of red *J–V* distortion as a function of different periods of white-light illumination. (c) Red *J–V* and (d) degree of red *J–V* distortion as a function of time after turning off white-light. Red *J–V* distortion is removed by illuminating with white-light for approximately 10 s, and red *J–V* distortion returns to maximum effect at approximately 1000 s after turning off white-light.

of the observed kink in the *J–V* curve. The red *J–V* distortion dynamics and its maximum distortion are related also to the interfacial defect properties, including defect density, distribution within the energy band gap, white-light intensity, and the electrical properties of window layer.

5. Conclusions

We have investigated the *J–V* characteristics of CISS devices with a solution processed silver nanowire composite window layer composed of silver nanowires embedded in indium tin oxide nanoparticles. Negatively charged deep level acceptor-like defects at the CdS/SNCW interface lead to crossover and red kink in the measured *J–V* characteristics of SNCW devices. Both crossover and red kink are removed by the photo-generation of holes in the CdS layer that neutralize the defects and produce a more favorable extraction configuration for photocurrent exiting the absorber material. The red *J–V* distortion gradually re-appears after turning off white-light because the defects become negatively charged again in the absence of photons with higher energy than the energy band gap of the CdS layer. Further studies on the physical origin of the CdS/SNCW interfacial defects, their characteristics, and the effects of the electrical properties of the SNCW layer on *J–V* curve distortion are still under investigation.

Acknowledgment

The authors like to acknowledge the financial support from the National Science Foundation (Fund no. ECCS-1202231).

References

[1] P. Jackson, D. Hariskos, E. Lotter, S. Paetel, R. Wuerz, R. Menner, W. Wischmann, M. Powalla, New world record efficiency for Cu(In,Ga)Se_2 thin-film solar cells beyond 20%, Prog. Photovoltaics: Res. Appl. 19 (2011) 894–897.

[2] I. Repins, M.A. Contreras, B. Egaas, C. DeHart, J. Scharf, C.L. Perkins, C. To, R. Noufi, 19.9%-efficient ZnO/CdS/CuInGaSe_2 solar cell with 81.2% fill factor, Prog. Photovoltaics: Res. Appl. 16 (2008) 235–239.

[3] T. Todorov, D.B. Mitzi, Direct liquid coating of chalcopyrite light-absorbing layers for photovoltaic devices, Eur. J. Inorg. Chem. 2010 (2010) 17–28.

[4] C.J. Hibberd, E. Chassaing, W. Liu, D.B. Mitzi, D. Linco, A.N. Tiwari, Non-vacuum methods for formation of Cu(In,Ga)$(Se,S)_2$ thin film photovoltaic absorbers, Prog. Photovoltaics: Res. Appl. 18 (2010) 434–452.

[5] S.E. Habas, H.A.S. Platt, M.F.A.M. van Hest, D.S. Ginley, Low-cost inorganic solar cells: from ink to printed device, Chem. Rev. 110 (2010) 6571–6594.

[6] M.A. Contreras, T. Barnes, J. van de Lagemaat, G. Rumbles, T.J. Coutts, C. Weeks, P. Glatkowski, I. Levitsky, J. Peltola, D.A. Britz, Replacement of transparent conductive oxides by single-wall carbon nanotubes in Cu(In,Ga)Se_2-based solar cells, J. Phys. Chem. C 11 (2007) 14045–14048.

[7] B. Brion, B. Lei, C.-H. Chung, W. Yang, W.-C. Hsu, H.-S. Duan, W.W.-J. Hou, S.-H. Li, Y. Yang. The development of hydrazine-processed Cu(In,Ga)$(Se,S)_2$ solar cells, Adv. Energy Mater. 2 (2012) 504-522.

[8] C.-H. Chung, T.-Z. Song, B. Bob, R. Zhu, H.-S. Duan, Y. Yang, Silver nanowire composite window layers for fully solution-deposited thin film photovoltaic devices, Adv. Mater. 24 (2012) 5499-5504.

[9] T. Eisenbarth, T. Unold, R. Caballero, C.A. Kaufmann, H.W. Schock, Interpretation of admittance, capacitance–voltage, and current–voltage signatures in Cu(In,Ga)Se_2 thin film solar cells, J. Appl. Phys. 107 (2010) 034509-1–034509-12.

[10] A. Niemegeers, M. Burgelman, R. Herberholz, U. Rau, D. Hariskos, H.W. Schock, Model for electronic transport in Cu(In,Ga)Se_2 solar cells, Prog. Photovoltaics: Res. Appl. 6 (1998) 407–421.

[11] M. Topic, F. Smole, J. Furlan, Examination of blocking current–voltage behaviour through defect chalcopyrite layer in ZnO/CdS/Cu(In,Ga)Se_2/Mo solar cell, Sol. Energy Mater. Sol. Cells 49 (1997) 311–317.

[12] I.L. Eisgruber, J.E. Granata, J.R. Sites, J. Hou, J. Kessler, Blue-photon modification of nonstandard diode barrier in $CuInSe_2$ solar cells, Sol. Energy Mater. Sol. Cells 53 (1998) 367-377.

[13] A.O. Pudov, J.R. Sites, M.A. Contreras, T. Nakada, H.W. Schock, CIGS *J–V* distortion in the absence of blue photons, Thin Solid Films 480–481 (2005) 273–278.

[14] A.O. Pudov, A. Kanevce, H.A. Al-Thani, J.R. Sites, F.S. Hasoon, Secondary barriers in CdS–$CuIn_{1-x}Ga_xSe_2$ solar cells, J. Appl. Phys. 97 (2005) 064901-1–064901-6.

[15] M. Kontges, R. Reineke-Koch, P. Nollet, J. Beier, R. Schaffler, J. Parisi, Light induced changes in the electrical behavior of CdTe and Cu(In,Ga)Se_2 solar cells, Thin Solid Films 403–404 (2002) 280–286.

[16] U. Rau, H.W. Schock, Electronic properties of Cu(In,Ga)Se_2 heterojunction solar cells – recent achievements, current understanding, and future challenges, Appl. Phys. A 69 (1999) 131–147.

[17] R. Scheer, H.W. Shock, Chalcogenide Photovoltaics: Physics, Technologies, and Thin Films Devices, Wiley-VCH Verlag GmbH & Co. KGaA ,Weinheim, Germany, 2011, 97–98.

[18] A. Niemegeers, M. Burgelman, A. De Vos, On the CdS/$CuInSe_2$ conduction band discontinuity, Appl. Phys. Lett. 67 (1995) 843–845.

[19] W.W. Hou, B. Bob, S.-H. Li, Y. Yang, Low-temperature processing of a solution-deposited CuInSSe thin-film solar cell, Thin Solid Films 517 (2009) 6853–6856.

[20] B. Lei, W.W. Hou, S.-H. Li, W. Yang, C.-H. Chung, Y. Yang, Cadmium ion soaking treatment for solution processed $CuInS_xSe_{2-x}$ solar cells and its effect on defect properties, Sol. Energy Mater. Sol. Cells 95 (2011) 2384–2389.

[21] C.-H. Chung, S.-H. Li, B. Lei, W. Yang, W.W. Hou, B. Bob, Y. Yang, Identification of the molecular precursors for hydrazine solution processed CuIn$(Se,S)_2$ films and their interactions, Chem. Mater. 23 (2011) 964–969.

[22] C.-H. Chung, B. Lei, S.-H. Li, B. Bob, W.W. Hou, H.-S. Duan, Y. Yang, Mechanism of sulfur incorporation into solution processed CuIn$(Se,S)_2$ films, Chem. Mater. 23 (2011) 4941–4946.